Stereospecific single step cyclization to give belt-functionalized pillar[6]arenes

Zeke Coady,[a] Jordan N. Smith,*[a] Katie A. Wilson[a,b] and Nicholas G. White*[a]

Two macrocycles were synthesized through cyclization reactions of secondary benzylic alcohols giving pillar[6]arenes with a methyl substituent at each belt position. These macrocycles form stereospecifically with the only observed isomer being the *rtctct* isomer with alternating up and down orientations of the belt methyl groups. Isolated yields were modest (7 and 9%) but the macrocycles are prepared in a single step from either a commercially-available alcohol or very readily-prepared precursor. X-ray crystal structures of the macrocycles indicate they have a capsule-like structure, which is far from the conventional pillar shape. Density functional theory calculations reveal that the energy barrier required to obtain the pillar conformation is significantly higher for these belt-functionalized macrocycles than for the conventional belt-unfunctionalized pillar[6]arenes.

Introduction

Since Ogoshi first reported the synthesis of pillar[5]arene (**P5**) in 2008,[1] interest in these soluble, readily-prepared macrocycles has grown dramatically.[2] Pillar[*n*]arenes have a rich host–guest chemistry, and this been used in a variety of applications including the formation of interlocked structures,[3–7] molecular separation of small aromatic compounds,[8,9] and catalysis.[10–13]

Numerous pillar[*n*]arenes have been reported containing a vast array of chemical functionalities, however the overwhelming majority of variation in pillar[*n*]arene structures have involved the rim groups (*i.e.* the OR groups in Figure 1).[14–18] Typically, substituents are either pre-installed at these positions and retained during cyclization, or a *per*-methoxy or *per*-ethoxy pillar[*n*]arene is synthesized, and then one or more alkyl group is removed allowing for subsequent functionalization.[2,19–22] This rim functionalization approach has two advantages: it is typically synthetically straight-forward, and it also typically does not impact the pillar-like geometry of the macrocycle.

In contrast to the frequent reports of rim-functionalized pillar[*n*]arenes, there have only been a handful of reports of functionalization at the aromatic ring,[23–27] or belt positions (also described as the "lateral" positions).[28–30] Notably, introduction of functional groups at the methylene carbon atoms induces chirality in the pillar[*n*]arenes and in the case of functionalization at multiple belt positions results in mixtures of configurational isomers (arising from the fact that each belt-substituent can be *cis* or *trans* to the adjacent substituent). The reported belt functionalizations have all involved **P5** and have either involved initial bromination or lithiation of the belt CH_2 groups. Five-fold bromination using *N*-bromosuccinimide (NBS) has been reported to give **Br$_5$-P5^{Me}** non-stereospecifically with one bromo group at each belt group (Figure 1),[28] although other authors have reported decomposition of **P5^{Me}** in the presence of NBS.[31] Mono-bromination with NBS followed by column chromatography on SiO_2 results in hydrolysis to give the mono-hydroxy derivative **OH-P5^{Et}**, which can subsequently be further functionalized.[30] Alternatively, reacting **P5** with benzophenone in the presence of *n*-BuLi followed by dehydration gives a macrocycle with an alkene functionality at one belt position.[29] While the number of compounds prepared through these approaches is very limited (Figure 1), they have found use for photophysical applications,[29,30,32–35] and in the synthesis of functional materials.[28,32,36–38]

While we are unaware of any reports of belt-functionalized pillar[6]arene (**P6**) macrocycles, Ma and co-workers recently reported that pillar[6]arene derivatives containing aryl groups directly attached to three of the belt positions could be synthesized *via* a stepwise synthesis. Two equivalents of 1,4-dimethoxybenzene were condensed with benzaldehyde derivatives to give dimers. Subsequent coupling of these dimers using paraformaldehyde gave the 1,3,5-trifunctionalized **P6** derivatives **Ar$_3$-P6^{Me}** non-stereospecifically, and these could then be further functionalized at the aryl groups (Figure 1).[39]

While belt-functionalized pillar[*n*]arenes have shown interesting properties, they have received relatively little attention. Perhaps most surprisingly, we are unaware of any reports of the synthesis of belt-functionalized pillar[*n*]arenes by a direct cyclization approach, *i.e*. by reaction of a 1,4-dialkoxybenzene with an aldehyde other than paraformaldehyde, or by direct reaction of an appropriate monomer such as a 1,4-dialkoxybenene featuring a secondary benzylic alcohol. Such a synthesis may provide an efficient route to interesting new macrocycles, and would also provide insight into the fundamental chemistry and structure of pillar[*n*]arenes. In this work, we investigate such syntheses and report the synthesis of two belt-*per*-methyl functionalized pillar[*n*]arenes through a single-step cyclization reaction.

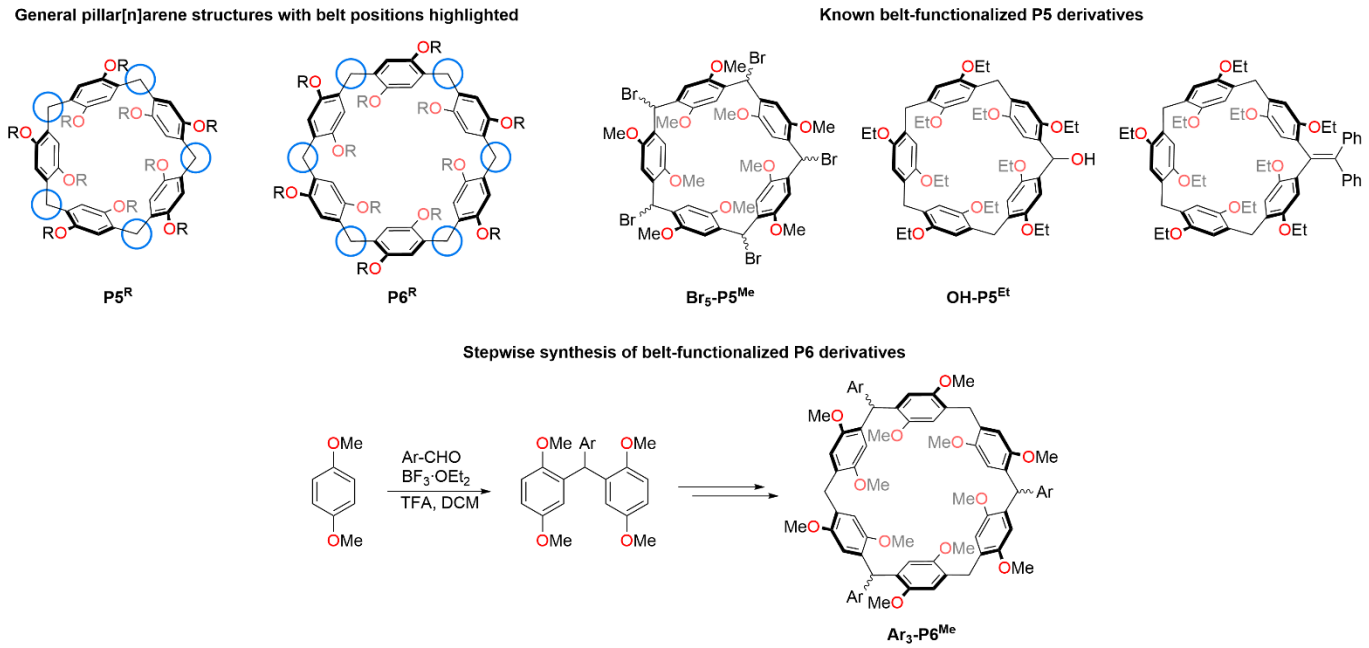

Figure 1 Structures of rim-functionalized pillar[*n*]arenes, **P5**^{R} and **P6**^{R}, with possible sites for belt-functionalization circled, known belt-functionalized **P5** derivatives and stepwise synthesis of 1,3,5-belt-functionalised **P6** derivatives (Ar = phenyl, 4-bromophenyl, 4-formylphenyl; the bromophenyl derivative was subsequently further functionalized after macrocycle formation).

Results and discussion

Synthesis of a belt-functionalized pillar[*n*]arene

We initially investigated the synthesis of pillar[*n*]arenes functionalized with one methyl group at each belt position directly from 1,4-diethoxybenzene (**1**) through a direct cyclization approach. That is, we attempted to react acetaldehyde and 1,4-diethoxybenzene in 1,2-dichloroethane in the presence of methanesulfonic acid (Scheme 1). When paraformaldehyde is used as the aldehyde source instead of acetaldehyde these conditions give high yields of *per*-ethoxy-pillar[5]arene (**P5**^{Et}). We conducted the reaction at 0 °C to minimize possible evaporation of acetaldehyde and observed that a reaction had taken place, giving a reaction mixture with a very complex ^{1}H NMR spectrum (Figure S32). There were large number of signals in the downfield region of the spectrum but apart from unreacted **1** (~ 30%) no major product could be identified. ESI-MS showed peaks with *m/z* of 983.5 and 1175.6, which match the expected Na^{+} adducts of the *per*-methyl-*per*-ethoxy pillar[5] and pillar[6]arenes **Me$_5$-P5**^{Et} and **Me$_6$-P6**^{Et}, suggesting that trace amounts of these compounds were formed.

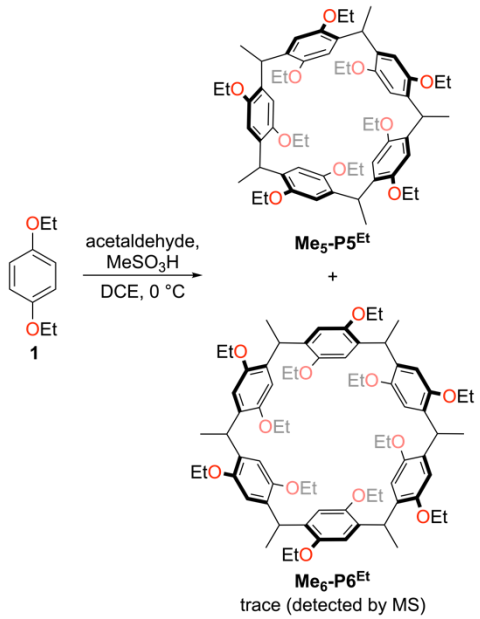

Scheme 1 Attempted direct synthesis of **Me$_5$-P5**^{Et} and **Me$_6$-P6**^{Et} from 1,4-diethoxybenzene.

Encouraged by this result, we next synthesized secondary alcohol **2** from **1** through a Friedel-Crafts acylation reaction to give ketone **3** followed by subsequent reduction (Scheme 2). Benzylic alcohols are believed to be intermediates during the formation of pillararenes, and unfunctionalized pillararenes have been prepared starting from primary benzylic alcohols.[40] We thought that starting from a secondary benzylic alcohol in which we have already formed one of the necessary carbon–carbon bonds between the aromatic ring and methylene group

may simplify the reaction and increase yields. Indeed, adding Lewis or Brønsted acids to **2** in dichloromethane (DCM) or 1,2-dichloroethane (DCE) did result in successful formation of **Me$_6$-P6^{Et}** (Scheme 2), albeit in modest yields. While some reactions gave mass spectra consistent with formation of some **Me$_5$-P5^{Et}** and a peak that could plausibly be the arylene resonance of this compound was observed in the ^{1}H NMR spectra of the crude reaction mixtures, we were never able to isolate this pentameric product.

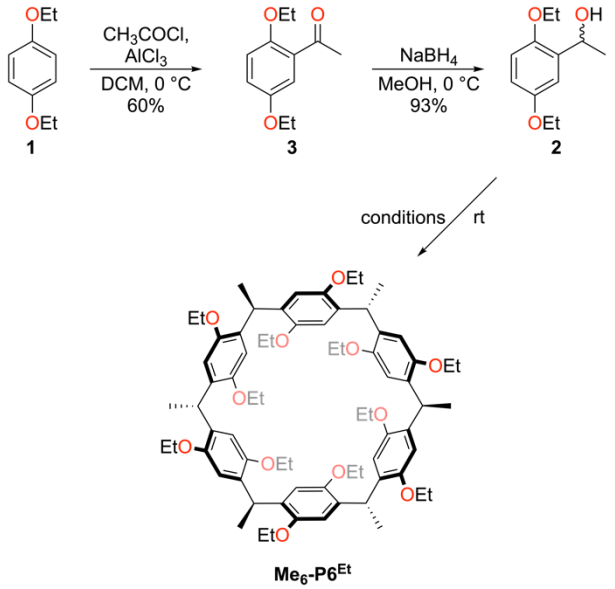

Scheme 2 Synthesis of belt-functionalized **Me$_6$-P6^{Et}**.

This initial screening suggested that methanesulfonic acid was the best choice of acid for these reactions (see later), so we conducted ^{1}H NMR studies to investigate formation of **Me$_6$-P6^{Et}** over time. We conducted these in CD_2Cl_2, $CDCl_3$ and DCE, adding three molar equivalents of $MeSO_3H$ to a 25 mM solution of **2** in the appropriate solvent. In all cases, complete disappearance of **2** was observed within an hour of addition of the acid, with broad peaks forming, consistent with soluble oligo/polymeric material (no precipitation was observed in any of these experiments). When the solvent was $CDCl_3$, no peaks corresponding to macrocyclic structures were ever observed.

In both DCM and DCE, a sharp peak at approximately 6.55 ppm appears within 24 hours, which we attribute to the arylene resonance of **Me$_6$-P6^{Et}**. Other peaks consistent with formation of the macrocycle are also apparent (spectra in CD_2Cl_2 are shown in Figure 2, and Figures S18 and S19). Integration of the ^{1}H NMR spectrum suggests that this resonance represents ~ 12% of the mixture after 48 hours in CD_2Cl_2, at which point little change is observed in the reaction spectra for several days before the concentration of **Me$_6$-P6^{Et}** appears to decrease after approximately one week. Integration of the ^{1}H NMR spectrum is slightly more difficult in DCE due to the difficulties in working in a non-deuterated solvent, but it seems that a similar or slightly larger amount of **Me$_6$-P6^{Et}** is formed in this solvent (Figure S22).

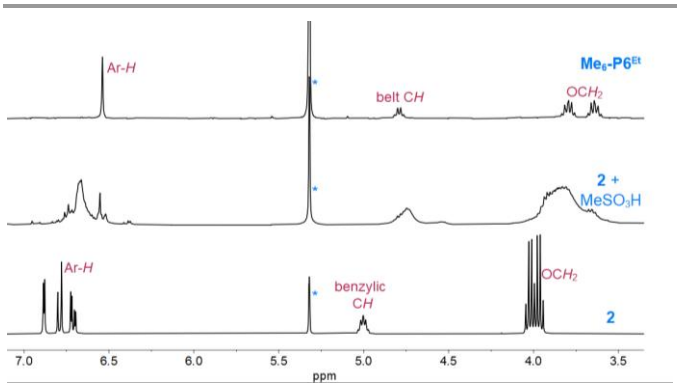

Figure 2 Partial ^{1}H NMR spectra of **2**, **Me$_6$-P6^{Et}**, and the reaction mixture 24 hours after mixing **2** with three equivalents of $MeSO_3H$. The spectra of **2** and the reaction mixture were recorded at 25 mM concentrations, the spectrum of **Me$_6$-P6^{Et}** is far more dilute, due to its limited solubility in this solvent (CD_2Cl_2, 400 MHz, 298 K).

In tandem with the *in situ* ^{1}H NMR studies, we screened a variety of other reaction conditions on larger scales for work-up and possible isolation. After aqueous work-up, the organic fraction was analyzed by ^{1}H NMR spectroscopy. Studies of reaction solvent and reaction time gave results consistent with the *in situ* ^{1}H NMR studies, *i.e.* DCE was a slightly better solvent than DCM, while chloroform gave no product, and stopping the reaction after three days gave the highest amount of product. Subsequently, we focused our studies on reactions left for three days in DCE: further studies in this solvent showed that heating the reaction to 75 °C resulted in minimal product formation. Investigating the choice of acid showed that neither *p*-toluenesulfonic acid nor trifluoroacetic acid gave any identifiable product. Aluminium chloride, sulfuric acid and triflic acid all gave some product, but none gave as high yields as those obtained with methanesulfonic acid (Table 1).

Table 1. Effect of acid on yield of Me$_6$-P6^{Et}.

Solvent	Catalyst	Time (h)	% yield[a]
1,2-DCE	*p*-TsOH	72	0
1,2-DCE	CF_3CO_2H	72	0
1,2-DCE	$AlCl_3$	72	1
1,2-DCE	H_2SO_4	72	4
1,2-DCE	CF_3SO_3	72	7
1,2-DCE	$MeSO_3H$	72	15 (9)[b]

[a] Approximate yields obtained from integration of ^{1}H NMR spectrum of crude reaction mixture after aqueous work-up. [b] Isolated yield given in parentheses.

Attempts to purify the reaction mixture using column chromatography on either alumina or silica were unsuccessful, with decomposition of the macrocycle apparent. However, it was possible to isolate pure **Me$_6$-P6^{Et}** from the reaction mixture by simply triturating with dichloromethane. This gave the compound in pure form in 9% isolated yield. The new macrocycle was characterized by ^{1}H and ^{13}C NMR spectroscopy, high resolution ESI mass spectrometry and X-ray crystallography.

Solid state structure of Me_6-P6^{Et}

Single crystals of **Me_6-P6^{Et}** were obtained by diffusing either pentane vapour or diethyl ether vapour into a chloroform solution of the macrocycle. Synchrotron X-ray crystallography revealed that the two are isostructural and so only the higher quality structure (obtained from diffusion of pentane) is discussed here (data for both structures are provided in the Supporting Information). Both structures appear to contain a chloroform solvate in the centre of the macrocycle, although this was difficult to model due to disorder (see Supporting Information).

The structure (Figure 3) shows that the introduction of six methyl groups around the ring of pillar[6]arene has very significant conformational consequences. Most notably, **Me_6-P6^{Et}** clearly does not have the expected pillar shape (which would result from a co-planar arrangement of the bridging carbon atoms). Instead, **Me_6-P6^{Et}** adopts a chair conformation analogous to cyclohexane (Figure 3c), with carbon atoms positioned ~0.76 Å above or below the mean plane. Continuing the cyclohexane analogy, the methyl groups at the belt are orientated equatorially, presumably to minimize steric interactions with the ethoxy groups. Similarly, the directionality of the arylene units alternates, unlike the pillar conformation of **P6^{R}** in which all arylene units are orientated in the same direction. Again, this conformation works to minimize steric interactions between the belt and rim ethoxy groups. The six arylene groups are twisted substantially, with opposite aryl rings parallel to one another. As a result, the macrocycle adopts a capsule-like structure, with three ethoxy groups blocking access to the top and bottom of the macrocycle (Figure 3b).

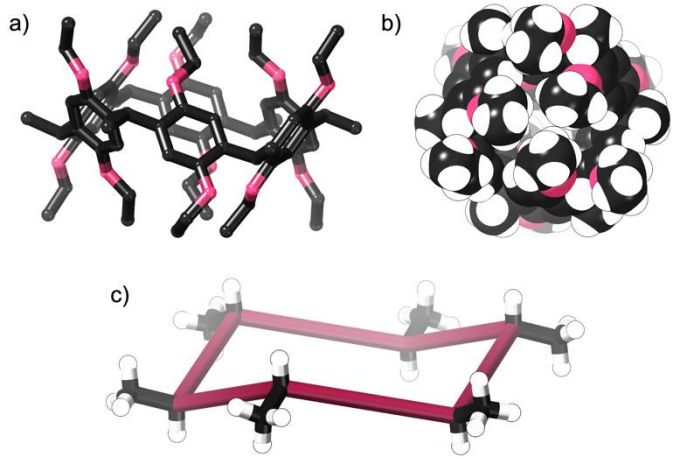

Figure 3 Views of the X-ray crystal structure of **Me_6-P6^{Et}**: a) side-on view of the structure, b) space-filling view of the macrocycle viewed from the top showing the ethoxy groups blocking access to the macrocycle cavity, c) view of the macrocycle with diethoxybenzene groups shown as a straight line, emphasizing chair-like structure.

Stereochemical analysis of Me_6-P6^{Et}

Similar to resorcinarenes[41] but unlike regular **P6^{R}**, the addition of alkyl groups at the bridging positions of pillararenes results in three stereochemical/configurational components that contribute to the overall stereochemistry (Figure 4):

i) the relative arrangement of the methyl groups at the bridging positions (Figure 4a), where each methyl group may be *cis* (*c*) or *trans* (*t*) relative to an arbitrarily chosen starting point (*r*). Of the eight possible non-enantiomeric arrangements *rccccc*, *rcccct*, *rccctt*, *rcctct*, *rctcct*, *rccttt*, *rcttct* and *rtctct* (see Figure S36), only the *rtctct* isomer is observed experimentally. This configuration is formed during the condensation and macrocyclization steps.

ii) the actual orientation of these methyl groups (axial or equatorial) due to the chair-like conformation of the macrocycle (Figure 4b). The arrangement depends on the configuration in point i); for the *rtctct* isomer this may be all-equatorial or all-axial. These could theoretically convert due to “chair flipping” behaviour analogous to cyclohexane, but for **Me_6-P6^{Et}** this process is expected to be very high in energy. Only the all-equatorial conformation is observed experimentally.

iii) the relative directionality of the arylene units (Figure 4c). Due to rotation of the aryl rings through the macrocycle, the alkyloxy groups may be individually orientated in the same or opposite directions. By arbitrarily defining a **+** sign to a rightwards tilt, the observed conformer is the **+–+–+–** arrangement. This conformation has been observed for other **P6** derivatives, although this is not common (see next Section). This conformation is independent of points i) or ii).

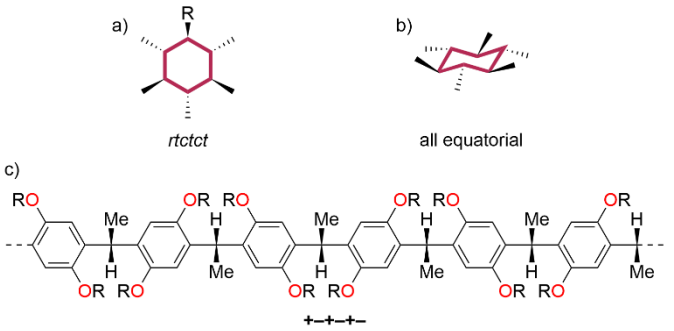

Figure 4 Stereochemical elements contributing to the overall stereochemistry of **Me_6-P6^{Et}**: a) the individual arrangement of the methyl groups at the bridge positions, b) the actual orientation of the methyl groups (axial or equatorial), and c) macrocycle projection demonstrating the orientation of the arylene groups. In a) and b) phenylene rings are represented as a bold maroon line.

Of the myriad of possible stereochemical outcomes from the macrocyclization, only the *rtctct*, all-equatorial, **+–+–+–** isomer is observed in the solid state. In solution, the ^{1}H NMR spectrum of **Me_6-P6^{Et}** shows a single species of high symmetry (Figure 2). The ethyloxy methylene protons are diastereotopic at 25°C (3.80 and 3.66 ppm), and fail to converge upon heating to 90 °C in d_8-toluene. This diastereotopicity contrasts with that of **P6^{Et}**, in which the ethyloxy methylene proton resonances appear homotopic due to rapid interconversion between enantiomeric pillar-conformers on the NMR timescale. These data are consistent with the *rtctct* isomer, but cannot exclude rapid interconversions between other conformers outlined in points ii) and iii).

The apparent absence of other isomers from the reaction mixtures speaks to the remarkable stereospecificity of the reaction, presumably as a result of reversibility targeting the

thermodynamic product. The selective formation of a hexameric **P6** macrocycle in DCE is unusual as this solvent typically templates smaller **P5** derivatives. We suggest that it arises from reduced strain of the alternating up/down, all-equatorial arrangement of the bridging methyl groups that is not possible for the pentamer.

Conformational analysis of P6^{R} and Me$_6$-P6^{R} derivatives

We undertook a search of the Cambridge Structural Database (CSD)[42] to compare the crystal structures of belt-functionalized pillararenes **Me$_6$-P6^{Et}** and **Me$_6$-P6^{Me}** (see later) with conventional pillar[*n*]arenes. This study is summarized here, with full details including visualization and analysis of the data provided in the Supporting Information. While pillar[*n*]arene macrocycles are nearly always drawn in their idealized pillar forms, *i.e.* with all aryl rings parallel to the central axis, this is not necessarily an accurate reflection of reality. Pillar[5]arenes do nearly always adopt this conformation, and visual inspection of the 365 X-ray crystal structures of these compounds containing atomic coordinates in the CSD shows that > 98% of these have the idealized pillar form. While there are only two crystal structures of belt-functionalized **P5^{R}** derivatives in the CSD, interestingly these both have a pillar-like geometry, despite the incorporation of very bulky diphenylethene[29] or fullerene[30] substituents at the belt position.

In contrast, crystal structures of pillar[6]arenes are often not pillar shaped. A search of the CSD revealed 61 structurally characterized **P6^{R}** macrocycles; initial visual inspection suggested that ~ 60% of these have the classic pillar shape. In an effort to come up with a more precise definition of a "pillar-shaped" pillar[*n*]arene, we looked at the arrangement of the alkoxy oxygen atoms in each structure. A total of 42 of the 61 **P6^{R}** structures have all oxygen atoms pointing in the same direction (*i.e.* **++++++** in Figure 4). These structures generally have the classical pillar shape, characterized by parallel or close-to-parallel aryl rings, although there are a small number of structures that show relatively large tilts for these rings. In these structures, adjacent aryl rings are close to parallel with only small deviations of the mean planes of adjacent arylene rings from the ideal pillar angle of 60° [mean deviation = 3.8(3)°]. The belt carbon atoms are generally co-planar or close-to-co-planar belt carbon atoms [mean deviation from plane = 0.11(1) Å].

The remaining 19 **P6^{R}** structures have three of the aryl rings "flipped" such that some of the alkoxy oxygen atoms point in a different direction to others giving the **+++−−−** or **+−+−+−** conformers (Figure 5). The **+++−−−** conformation (12 structures in CSD) takes on a geometry in which most aryl rings are close to parallel, but significantly tilted in one direction resulting in mean plane angles between arylene rings that are further from 60° [mean deviation = 9.8(5)°] and reduced co-planarity of the belt carbon atoms [mean deviation from plane = 0.30(2) Å]. There are seven structures with the **+−+−+−** geometry; in this geometry the rings are staggered and far from parallel [mean deviation from 60° = 21(1)°] and the belt carbon atoms are typically far from co-planar [mean deviation from plane = 0.66(3) Å]. These significant distortions mean that this conformer of **P6** bears essentially no resemblance to a pillar.

Me$_6$-P6^{Et} and **Me$_6$-P6^{Me}** adopt the **+−+−+−** conformation and have similar structural parameters to belt-unsubstituted **+−+−+−** structures [mean deviation of adjacent rings from 60° = 25.7(3)°, mean deviation from co-planarity = 0.78(1) Å]. The only notable difference between **Me$_6$-P6^{R}** and other **+−+−+−** pillar[6]arenes is in the angles around the belt carbon atoms, *i.e.* the $C_{arylene}$–C_{belt}–$C_{aryllene}$ angles. These are quite close to the ideal tetrahedral angle of 109.47° in the structures of **Me$_6$-P6^{R}** [mean deviation = 2.4(3)°], while all conformers of belt-unsubstituted **P6^{R}** structures have significantly greater deviations from tetrahedral angles [mean deviations = 4.8(1)° for **++++++**, 5.4(2)° for **+++−−−**, 5.0(3)° for **+−+−+−**]. Presumably the additional steric bulk introduced by the methyl substituent in **Me$_6$-P6^{R}** macrocycles enforces a more rigidly tetrahedral geometry at the belt carbon atom.

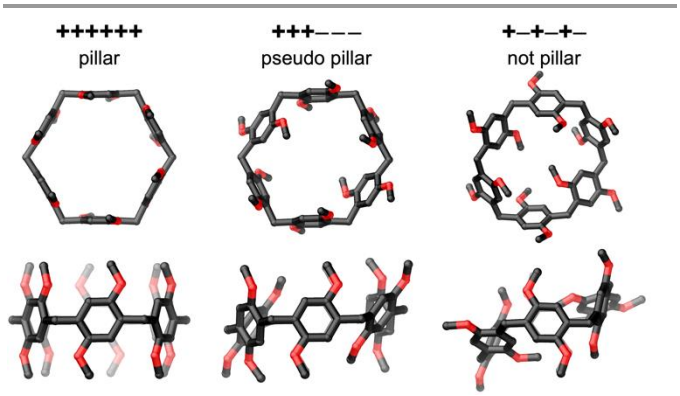

Figure 5 Representative structures of **P6^{Et}** in the CSD (ethyl substituents truncated and hydrogen atoms omitted for clarity; CSD codes: **++++++** = TASQOW,[8] **+++−−−** = WIHRUD,[43] **+−+−+−** = TASQOW02 [9]).

We undertook computational calculations to investigate this further. The **P6^{Et}** structures used in Figure 5 were used as starting points for DFT calculations [ωB97xD/6-311++g(2df,2p)//ωB97xD/6-31g(d,p)]. These revealed that in the gas phase the **++++++** conformer is 31 kJ mol^{-1} higher in energy than the **+−+−+−** conformer and 29 kJ mol^{-1} higher in energy than the **+++−−** conformer. *I.e.* the **+++−−** and **+−+−+−** conformers have essentially the same energy, but the pillar-like **++++++** conformer is ~ 30 kJ mol^{-1} higher. We note that these gas phase calculations do not include solvent/guest molecules, which may increase the favorability of the pillar form. Similar calculations by Zuilhof and co-workers,[44] reported while this work was in progress, give broadly similar results.[45]

In contrast to the relatively low energy barrier between the conformers of belt-unfunctionalized pillar[6]arenes, the energy barrier required for **Me$_6$-P6^{Et}** to reach a pillar-like **++++++** form (Figure S45) is significantly higher, with the **++++++** conformer being 83 kJ mol^{-1} higher in energy that the **+−+−+−** conformation. We suggest that the additional steric demands introduced by the belt methyl substituents restrict the geometry of these groups.

Solution binding of Me$_6$-P6^{Et}

We conducted an initial screen of the ability of **Me$_6$-P6^{Et}** to bind guests using qualitative ^{1}H NMR experiments in $CDCl_3$. The

new macrocycle showed no binding of 1,2-tropylium tetrafluoroborate in this solvent (this molecule binds strongly to **P6^{Et}** [46]). We also observed no evidence of binding of tetrabutylammonium hexafluorophosphate (similar alkylammonium guests bind to **P6^{sBu}** [47]) or of DCE. The crystal structure of **Me$_6$-P6^{Et}** suggests it might be large enough to accommodate a small cationic guest such as the tetramethylammonium cation, however no evidence of binding of tetramethylammonium tetraphenylborate was observed in 1:1 $CDCl_3$:d_6-acetone (solvent mixture used for solubility reasons). We reasoned that the structure of the macrocycle might present a kinetic barrier to binding, but even after extended heating (60 hours at 55 °C) there was no evidence of encapsulation. While studies are somewhat limited by the solubility of **Me$_6$-P6^{Et}**, which require the use of chlorinated solvents, our initial screen suggests that this macrocycle does not bind to "traditional" guests for belt-unsubstituted pillar[*n*]arenes.

Attempts to form other laterally functionalized pillar[*n*]arenes

Belt substitution: We attempted to form other belt-functionalized pillar[*n*]arenes containing additional functionality at the belt. We investigated the direct cyclization of **1** with propanal, octanal or benzaldehyde at room temperature using methanesulfonic acid in 1,2-dichloroethane but did not observe any evidence for macrocycle formation.[48] When propanal or octanal were used, we observed formation of the competing aldol product. To mitigate this, and to try and make formation of a macrocycle more probable, we pre-formed secondary alcohol **4** using a similar approach to that used to prepare **2** (synthesis given in Supporting Information). When we subjected **4** to the optimized reaction conditions developed to prepare **Me$_6$-P6^{Et}**, we did not observe formation of **Et$_6$-P6^{Et}** by ^{1}H NMR spectroscopy or mass spectrometry. Instead, the ^{1}H NMR spectrum of the crude reaction mixture showed a mixture of **1** and dimeric product **5** in a 1:2 ratio (Scheme 3). These two components made up approximately half of the reaction products, with the remaining compounds unidentified. The inability to form **Et$_6$-P6^{Et}** is consistent with either reduced favorability of macrocycle formation (possibly due to increased steric demands from the ethyl substituent) or to a greater favorability of the aldol reaction product sequestering the aldehyde component, presumably through a *retro*-Friedel-Crafts type process (see Scheme S3).

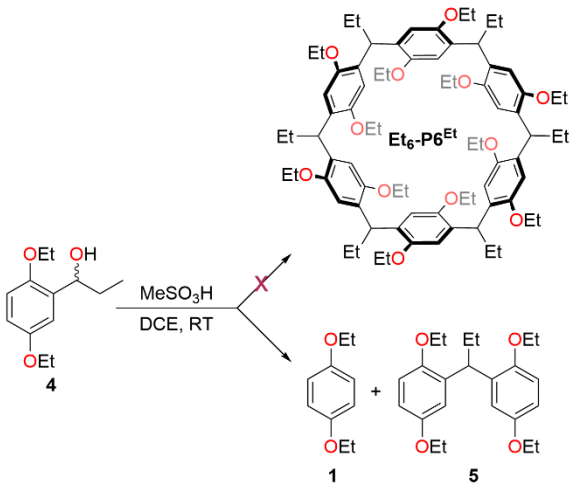

Scheme 3 Attempted synthesis of belt-functionalized **Et$_6$-P6^{Et}**.

Rim substitution: We investigated the effect of different rim substituents on the formation of laterally functionalized pillar[*n*]arenes by studying the cyclization of commercially available **6** containing methoxy groups, as well as **7** containing hexyloxy groups (Scheme 4, synthesis given in the Supporting Information). Initial studies were carried out using ^{1}H NMR experiments, which suggested the formation of **Me$_6$-P6^{Me}** from **6** in CD_2Cl_2 and DCE, but not in $CDCl_3$, *i.e.* very similar results to those observed for **Me$_6$-P6^{Et}**. When these NMR scale experiments were conducted on hexyloxy-substituted **7**, no evidence for formation of **Me$_6$-P6^{hex}** was observed by either ^{1}H NMR spectroscopy or mass spectrometry (see Supporting Information). We suggest that the larger hexyloxy rim substituents prevent the macrocycle reaching the favored **+–+–+–+–** form (due to steric clashes of the hexyl groups) and thus prevents cyclization.

The synthesis of **Me$_6$-P6^{Me}** was then repeated on a preparative scale using the optimized conditions developed for **Me$_6$-P6^{Et}**. The methoxy macrocycle **Me$_6$-P6^{Me}** was isolated in 7% yield by simple precipitation with DCM. In this case, the macrocycle was slightly impure (~ 90% purity, as estimated by ^{1}H NMR spectroscopy), and had even lower solubility than **Me$_6$-P6^{Et}**. Attempts to purify the macrocycle further by chromatography were unsuccessful, and recrystallization had only limited success (see Supporting Information), and due to its very low solubility we were not able to study its guest binding properties. We were able to obtain single crystals of **Me$_6$-P6^{Me}** (Figure 4), which again is the *rtctct* isomer, as expected based on NMR analysis. In the solid state, it adopts an almost identical structure to that of **Me$_6$-P6^{Et}**, with a **+–+–+–** conformation that is far from pillar-like (see Supporting Information for structural analysis).

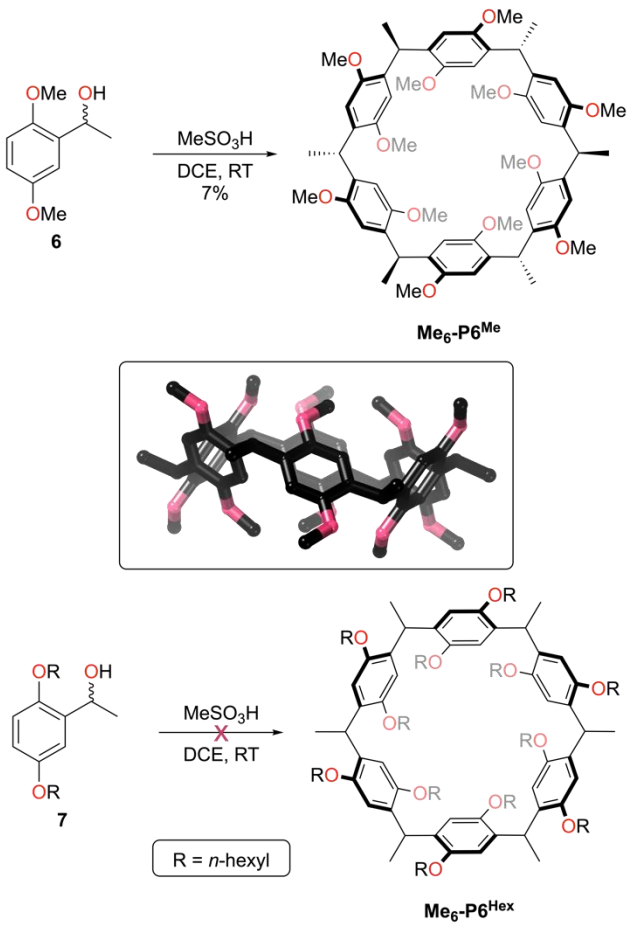

Scheme 4 Synthesis of belt-functionalized pillar[6]arene **Me$_6$-P6^{Me}** and attempted synthesis of **Me$_6$-P6^{hex}**. The X-ray crystal structure of **Me$_6$-P6^{Me}** is shown inset (hydrogen atoms and solvent molecules omitted for clarity).

Discussion

A seemingly relatively minor alteration to pillar[*n*]arene structure—the replacement of hydrogen atoms at the belt positions with methyl groups—results in dramatic changes to macrocycle synthesis and structure. In terms of synthesis, negligible formation of pentameric macrocycles is observed even in dichloromethane, which typically favors this isomer, yields are relatively low, and macrocycle formation is much slower than for typical pillar[*n*]arene syntheses (several days for reactions to form **Me$_6$-P6^{R}** to reach equilibrium rather than a few minutes for conventional pillar[*n*]arenes[49]). In terms of structure, addition of the methyl groups introduces the possibility of eight different non-enantiomeric isomers, of which only a single one is isolated. The methyl groups also impact the conformation of the macrocycles, with the **+–+–+–** conformation being preferred.

It is interesting that although all reaction components stay soluble, and thus there is no loss of equilibrium due to precipitation,[50] yields are low, and we attribute this to the sheer unlikeliness of forming significant amounts of the acyclic hexamer with the right arrangement of methyl groups. Attempts to leave the reactions for longer to increase yields were unsuccessful, presumably due to irreversible side-reactions eventually degrading the macrocycle. We note that we did not investigate stringently anhydrous/anaerobic conditions, which may minimize side-reactions. Forming a pentameric macrocycle would require at least two adjacent methyl groups to be *cis* to one another and we suggest that the strain induced by this precludes formation of significant amounts of the **Me$_5$-P5^{R}** macrocycles.

Attempts to introduce larger belt substituents were unsuccessful, which we attribute to competing aldol reactions sequestering the aldehyde. Attempts to introduce hexyl rim substituents were also unsuccessful, which we attribute to steric clashes of the hexyl groups caused by the **+–+–+–** conformation of the pre-macrocycle. Further studies with secondary alcohols that cannot form enolizable aldehydes may enable the synthesis of a greater range of belt-substituted macrocycles. Generally, if synthetic conditions could be found that overcome the barrier to achieving the pillar-like conformation while still favoring macrocyclization over oligomerization/polymerization, this may allow access to a wide range of macrocycles that may have interesting host–guest chemistry.

Conclusions

We report the stereoselective synthesis of two new belt-functionalized pillararenes, **Me$_6$-P6^{Me}** and **Me$_6$-P6^{Et}**. To the best of our knowledge, this is the first report of belt-functionalized pillar[n]arenes prepared in a single step cyclization, *i.e.* by "direct" synthesis rather than a step-wise construction of the macrocyclic ring or by modification of a belt-unfunctionalized pillar[n]arene. X-ray crystallographic studies reveal that both macrocycles have capsule-like **+–+–+–** conformations in the solid state with significant distortions from a conventional pillar-like geometry. Computational calculations indicate that the introduction of methyl groups at the belt positions significantly increases the energy barrier required to achieve the pillar geometry.

Macrocyclization yields were relatively low. This does not result from precipitation of oligomeric/polymeric material,[50] but instead may result from difficulties in the intermediate oligomer reaching the necessary *rtctct* configuration to allow cyclization. While the Friedel-Crafts reactions required to build up the oligomer are known to be reversible,[51] which will presumably allow for conversion between isomers, the statistical improbability of achieving this isomer presumably accounts for the low yield and long reaction times.

Attempts to introduce other groups at the belt position were hampered by competing aldol reactions, while attempts to incorporate large hexyl groups at the rim positions were unsuccessful, potentially due to steric clashes. The simple synthesis of these two new macrocycles indicates that even though there has been considerable research into pillar[*n*]arene macrocycles, there is still a significant amount of synthetic space that remains unexplored. We suggest that there are plenty of pillar[*n*]arene-related macrocycles waiting to be discovered.

Experimental Section

General remarks

Compound **1** was prepared as previously described,[52] compound **6** was purchased from Ambeed. The synthesis of alcohols **4** and **7** is described in the Supporting Information. Details of instrumentation, X-ray crystallography, computational calculations and characterization data are provided in the Supporting Information.

1-(2,5-diethoxyphenyl)ethanone (3)

Compound **1** (2.49 g, 15.0 mmol) and acetyl chloride (1.60 mL, 1.77 g, 22.5 mmol) were dissolved in DCM (10 mL) and cooled to 0 °C. Aluminium chloride (2.20 g, 16.5 mmol) was added portionwise under a nitrogen atmosphere and then the mixture was stirred under nitrogen at 0 °C for 3 hours during which time it rapidly turned a bright orange before turning red-brown and then dark brown. It was then added to a mixture of ice (~ 50 mL) and conc. $HCl_{(aq)}$ (10 mL) and left to warm to room temperature over an hour. The mixture was extracted with DCM (3 × 20 mL) and then the combined organic layers were washed with $NaOH_{(aq)}$ (2.0 M, 2 × 20 mL), water (20 mL) and dried ($MgSO_4$). Evaporation to dryness under reduced pressure gave **3** as an orange oil of approximately 95% purity (according to ^{1}H NMR spectroscopy). This material was purified by column chromatography (silica, 3:2 dichloromethane:petroleum spirits to neat dichloromethane) to give **3** as a yellow oil, which solidified upon standing. Yield: 1.87 g (8.99 mmol, 60%).

^{1}H NMR ($CDCl_3$): 7.29 (d, *J* = 3.2 Hz, 1H), 7.00 (dd, *J* = 9.0, 3.2 Hz, 1H), 6.87 (d, *J* = 9.0 Hz, 1H), 4.08 (q, *J* = 7.0 Hz, 2H), 4.01 (q, *J* = 7.0 Hz, 2H), 2.63 (s, 3H), 1.45 (t, *J* = 7.0 Hz, 3H), 1.38 (t, *J* = 7.0 Hz, 3H) ppm. ^{13}C{^{1}H} NMR ($CDCl_3$): 199.6, 153.0, 152.7, 128.8, 121.2, 114.6, 114.2, 64.8, 64.2, 32.2, 15.04, 14.98 ppm. HRESI-MS (pos.): 209.1172, calc. for $[C_{12}H_{16}O_3{\cdot}H]^+$ = 209.1172 Da.

1-(2,5-diethoxyphenyl)ethan-1-ol (2)

Ketone **3** (1.04 g, 5.00 mmol) was dissolved in methanol (25 mL) and cooled to 0 °C. $NaBH_4$ (0.21 g, 5.5 mmol) was added portionwise over approximately 2 minutes under a nitrogen atmosphere, and then the mixture was stirred under nitrogen at 0 °C for 10 minutes and then allowed to warm to room temperature over 2 hours. The mixture was diluted with ethyl acetate (50 mL), washed with $HCl_{(aq)}$ (1.0 M, 2 × 50 mL), then brine (50 mL), dried ($MgSO_4$) and then taken to dryness under reduced pressure to give **2** as a yellow oil. Yield: 0.969 g (4.61 mmol, 92%).

^{1}H NMR ($CDCl_3$): 6.91 (d, *J* = 2.9 Hz, 1H), 6.72 – 6.79 (m, 2H), 5.04 (q, *J* = 6.5 Hz, 1H), 4.03 (q, *J* = 7.0 Hz, 2H), 3.99 (q, *J* = 7.0 Hz, 2H), 2.80 (br. s, 1H), 1.50 (d, *J* = 6.5 Hz, 3H), 1.42 (t, *J* = 7.0 Hz, 3H), 1.39 (t, *J* = 7.0 Hz, 3H) ppm. ^{13}C{^{1}H} NMR ($CDCl_3$): 153.1, 150.2, 134.8, 113.4, 113.2, 112.5, 67.0, 64.3, 64.1, 23.0, 15.2, 15.1 ppm. HRESI-MS (pos.): 233.1143, calc. for $[C_{12}H_{18}O_3{\cdot}Na]^+$ = 233.1148 Da.

Me$_6$-P6^{Et}

Compound **1** (0.105 g, 0.500 mmol) was dissolved in 1,2-DCE (20 mL). Methanesulfonic acid (0.097 mL, 0.14 g, 1.50 mmol, 3.0 equiv.) was added and the mixture stirred at room temperature for 72 hours under a nitrogen atmosphere. The reaction was then quenched with water (10 mL) and basified by addition of $K_2CO_{3(aq)}$ (10 wt. %, 2 mL). The organic layer was separated and the aqueous layer extracted with 1,2-DCE (2 × 5 mL). The organic fractions were combined, dried ($MgSO_4$), and then concentrated on a rotary evaporator. DCM (3 mL) was added to the resulting brown solid, giving a brown solution and white solid. The suspension was sonicated and then heated to boiling (the compound did not dissolve upon heating). After cooling in a –18 °C freezer, the resulting solid was isolated by filtration, washed with DCM (2 × 1 mL), and thoroughly air-dried to give **Me$_6$-P6^{Et}** as white flakes. Yield: 0.0084 g (0.0073 mmol, 9%).

^{1}H NMR ($CDCl_3$, 400 MHz): 6.55 (s, 12H), 4.82 (q, *J* = 7.1 Hz, 6H), 3.77 – 3.84 (m, 12 H), 3.61 – 3.69 (m, 12H), 1.43 (d, *J* = 7.1 Hz, 18H), 1.16 (t, *J* = 7.0 Hz, 36 H). ^{13}C{^{1}H} NMR ($CDCl_3$, 101 MHz): 150.3, 133.7, 112.9, 64.7, 30.9, 20.7, 15.1 ppm. HRESI-MS (pos.) 1175.6799, calc. for $[C_{72}H_{96}O_{12}{\cdot}Na]^+$ = 1175.6798 Da.

Me$_6$-P6^{Me}

Compound **4** (0.364 g. 2.00 mmol) was dissolved in 1,2-DCE (80 mL). Methanesulfonic acid (0.39 mL, 0.57 g, 6.0 mmol) was added and the mixture stirred at room temperature for 72 hours under a nitrogen atmosphere. The reaction was then quenched with water (20 mL) and then $K_2CO_{3(aq)}$ (10 wt. %, 5 mL). The organic layer was separated and the aqueous layer extracted with DCM (2 × 20 mL). The organic fractions were combined, dried ($MgSO_4$), and then concentrated on a rotary evaporator. DCM (5 mL) was added to the resulting brown solid, giving a brown solution and white solid. The suspension was sonicated and then heated to boiling (the compound did not dissolve upon heating) After cooling in a –18 °C freezer, the resulting solid was isolated by filtration, washed with DCM (2 × 1 mL), and dried *in vacuo* to give **Me$_6$-P6^{Me}** of approximately 90% purity as a white powder. Yield: 0.0024 g (0.025 mmol, 7%).

^{1}H NMR ($CDCl_3$, 400 MHz): 6.56 (s, 12H), 4.78 (q, *J* = 7.0 Hz, 6H), 3.52 (s, 36 H), 1.47 (d, *J* = 6.9 Hz, 18H). ^{13}C{^{1}H} NMR ($CDCl_3$, 101 MHz): 151.2, 133.5, 112.0, 56.7, 31.0, 20.5 ppm. HRESI-MS (pos.): 1007.4900, calc. for $[C_{60}H_{72}O_{12}{\cdot}Na]^+$ = 1007.4916 Da.

Computational calculations

DFT calculations were performed using ωB97xD/6-311++g(2df,2p)//ωB97xD/6-31g(d,p) as implemented in Gaussian 16.[53] All reported energies include the zero-point vibrational energy correction (scale factor= 0.9756).[54] Gas phase energies for different geometries of belt-unfunctionalized **P6^{Et}** structures were calculated using representative X-ray crystal structures as the starting points (CSD: TAZQOW for **++++++**,[8] CSD: WIHRUD for **+++−−−**,[43] CSD: TAZQOW02 for **+−+−+−**[9]). Energies for different geometries of **Me$_6$-P6^{Et}** were calculated using the X-ray crystal structure as a starting point

for the **+–+–+–** geometry, and by modifying dihedral angles of the **+–+–+–** geometry to create a pillar-like **++++++** geometry. All **P6^{Et}** and **Me$_6$-P6^{Et}** structures remained in the input starting geometry upon minimization (*e.g.* **++++++** conformer remained **++++++** after minimization). Atomic coordinates for all structures have been provided as .xyz files (Supporting Information).

Author addresses

[a] Research School of Chemistry
Australian National University
Canberra, ACT, Australia, 2601
Email: nicholas.white@anu.edu.au

[b] Department of Biochemistry
Memorial University of Newfoundland
St. John's, NL, Canada, A1C 5S7

Acknowledgements

We thank Dr Michael Gardiner (ANU) for assistance with synchrotron X-ray crystallography, and Dr Douglas Lawes (ANU) for assistance with NMR spectroscopy. We thank the Australian Research Council for financial support (DP200100535). Parts of this work were conducted using the MX1 beamline at the Australian Synchrotron.[55] All calculations were performed with the assistance of resources and services from the National Computational Infrastructure (NCI), which is supported by the Australian Government. We thank Prof. Megan O'Mara for helpful discussions, funding acquisition and support, and providing access to the NCI.

References

(1) Ogoshi, T.; Kanai, S.; Fujinami, S.; Yamagishi, T.; Nakamoto, Y. *Para* -Bridged Symmetrical Pillar[5]Arenes: Their Lewis Acid Catalyzed Synthesis and Host–Guest Property. *J. Am. Chem. Soc.* **2008**, *130* (15), 5022–5023.

(2) Ogoshi, T.; Yamagishi, T.; Nakamoto, Y. Pillar-Shaped Macrocyclic Hosts Pillar[*n*]Arenes: New Key Players for Supramolecular Chemistry. *Chem. Rev.* **2016**, *116* (14), 7937–8002.

(3) Strutt, N. L.; Forgan, R. S.; Spruell, J. M.; Botros, Y. Y.; Stoddart, J. F. Monofunctionalized Pillar[5]Arene as a Host for Alkanediamines. *J. Am. Chem. Soc.* **2011**, *133* (15), 5668–5671.

(4) Ogoshi, T.; Yamafuji, D.; Aoki, T.; Yamagishi, T. Thermally Responsive Shuttling Behavior of a Pillar[6]Arene-Based [2]Rotaxane. *Chem. Commun.* **2012**, *48* (54), 6842.

(5) Zhang, Z.; Han, C.; Yu, G.; Huang, F. A Solvent-Driven Molecular Spring. *Chem. Sci.* **2012**, *3* (10), 3026.

(6) Li, S.-H.; Zhang, H.-Y.; Xu, X.; Liu, Y. Mechanically Selflocked Chiral Gemini-Catenanes. *Nat. Commun.* **2015**, *6* (1), 7590.

(7) Kato, K.; Fa, S.; Ohtani, S.; Shi, T.; Brouwer, A. M.; Ogoshi, T. Noncovalently Bound and Mechanically Interlocked Systems Using Pillar[*n*]Arenes. *Chem. Soc. Rev.* **2022**, *51* (9), 3648–3687.

(8) Jie, K.; Liu, M.; Zhou, Y.; Little, M. A.; Bonakala, S.; Chong, S. Y.; Stephenson, A.; Chen, L.; Huang, F.; Cooper, A. I. Styrene Purification by Guest-Induced Restructuring of Pillar[6]Arene. *J. Am. Chem. Soc.* **2017**, *139* (8), 2908–2911.

(9) Jie, K.; Liu, M.; Zhou, Y.; Little, M. A.; Pulido, A.; Chong, S. Y.; Stephenson, A.; Hughes, A. R.; Sakakibara, F.; Ogoshi, T.; Blanc, F.; Day, G. M.; Huang, F.; Cooper, A. I. Near-Ideal Xylene Selectivity in Adaptive Molecular Pillar[*n*]Arene Crystals. *J. Am. Chem. Soc.* **2018**, *140* (22), 6921–6930.

(10) Ogoshi, T.; Ueshima, N.; Yamagishi, T. An Amphiphilic Pillar[5]Arene as Efficient and Substrate-Selective Phase-Transfer Catalyst. *Org. Lett.* **2013**, *15* (14), 3742–3745.

(11) Yao, Y.; Xue, M.; Zhang, Z.; Zhang, M.; Wang, Y.; Huang, F. Gold Nanoparticles Stabilized by an Amphiphilic Pillar[5]Arene: Preparation, Self-Assembly into Composite Microtubes in Water and Application in Green Catalysis. *Chem. Sci.* **2013**, *4* (9), 3667.

(12) Wanderlind, E. H.; Liz, D. G.; Gerola, A. P.; Affeldt, R. F.; Nascimento, V.; Bretanha, L. C.; Montecinos, R.; Garcia-Rio, L.; Fiedler, H. D.; Nome, F. Imidazole-Functionalized Pillar[5]Arenes: Highly Reactive and Selective Supramolecular Artificial Enzymes. *ACS Catal.* **2018**, *8* (4), 3343–3347.

(13) Wang, K.; Jordan, J. H.; Velmurugan, K.; Tian, X.; Zuo, M.; Hu, X.-Y.; Wang, L. Role of Functionalized Pillararene Architectures in Supramolecular Catalysis. *Angew. Chem. Int. Ed.* **2021**, *60* (17), 9205–9214.

(14) Ogoshi, T.; Shiga, R.; Yamagishi, T. Reversibly Tunable Lower Critical Solution Temperature Utilizing Host–Guest Complexation of Pillar[5]Arene with Triethylene Oxide Substituents. *J. Am. Chem. Soc.* **2012**, *134* (10), 4577–4580.

(15) Guo, M.; Wang, X.; Zhan, C.; Demay-Drouhard, P.; Li, W.; Du, K.; Olson, M. A.; Zuilhof, H.; Sue, A. C.-H. Rim-Differentiated C_5 -Symmetric Tiara-Pillar[5]Arenes. *J. Am. Chem. Soc.* **2018**, *140* (1), 74–77.

(16) Ruengsuk, A.; Khamphaijun, K.; Pananusorn, P.; Docker, A.; Tantirungrotechai, J.; Sukwattanasinitt, M.; Harding, D. J.; Bunchuay, T. Pertosylated Pillar[5]Arene: Self-Template Assisted Synthesis and Supramolecular Polymer Formation. *Chem. Commun.* **2020**, *56* (62), 8739–8742.

(17) Tian, Y.; Guo, Y.; Dong, X.; Wan, X.; Cheng, K.-H.; Chang, R.; Li, S.; Cao, X.; Chan, Y.-T.; Sue, A. C.-H. Synthesis of Covalent Organic Pillars as Molecular Nanotubes with Precise Length, Diameter and Chirality. *Nat. Synth.* **2023**, *2*, 395–402.

(18) Kato, K.; Kaneda, T.; Ohtani, S.; Ogoshi, T. Per-Arylation of Pillar[*n*]Arenes: An Effective Tool to Modify the Properties of Macrocycles. *J. Am. Chem. Soc.* **2023**, *145* (12), 6905–6913.

(19) Cao, D.; Kou, Y.; Liang, J.; Chen, Z.; Wang, L.; Meier, H. A Facile and Efficient Preparation of Pillararenes and a Pillarquinone. *Angew. Chem. Int. Ed.* **2009**, *48* (51), 9721–9723.

(20) Ogoshi, T.; Demachi, K.; Kitajima, K.; Yamagishi, T. Monofunctionalized Pillar[5]Arenes: Synthesis and Supramolecular Structure. *Chem. Commun.* **2011**, *47* (25), 7164.

(21) Ogoshi, T.; Yamafuji, D.; Kotera, D.; Aoki, T.; Fujinami, S.; Yamagishi, T. Clickable Di- and Tetrafunctionalized Pillar[*n*]Arenes (*n* = 5, 6) by Oxidation–Reduction of Pillar[*n*]Arene Units. *J. Org. Chem.* **2012**, *77* (24), 11146–11152.

(22) Strutt, N. L.; Zhang, H.; Schneebeli, S. T.; Stoddart, J. F. Functionalizing Pillar[*n*]Arenes. *Acc. Chem. Res.* **2014**, *47* (8), 2631–2642.

(23) Strutt, N. L.; Zhang, H.; Schneebeli, S. T.; Stoddart, J. F. Amino-Functionalized Pillar[5]Arene. *Chem. Eur. J.* **2014**, *20* (35), 10996–11004.

(24) Bojtár, M.; Simon, A.; Bombicz, P.; Bitter, I. Expanding the Pillararene Chemistry: Synthesis and Application of a 10 + 1 Functionalized Pillar[5]Arene. *Org. Lett.* **2017**, *19* (17), 4528–4531.

(25) Kiruthika, J.; Srividhya, S.; Arunachalam, M. Anion-Responsive Pseudo[3]Rotaxane from a Difunctionalized Pillar[4]Arene[1]Quinone and a Bis-Imidazolium Cation. *Org. Lett.* **2020**, *22* (20), 7831–7836.

(26) Wang, Z.; Liu, Y. A.; Yang, H.; Hu, W.-B.; Wen, K. *Ortho* -Functionalization of Pillar[5]Arene: An Approach to Mono-*Ortho* -Alkyl/Aryl-Substituted A1/A2-Dihydroxypillar[5]Arene. *Org. Lett.* **2022**, *24* (9), 1822–1826.

(27) Wang, H.; Thikekar, T. U.; Xue, J.; Zhu, Y.; Fang, W.; Xu, J.; Sue, A. C.-H.; Zhao, H. Synthesis, Structures, and Conformational Characteristics of Pillararene-Based Diels–Alder Adducts with Embedded Chiral Centres. *Org. Chem. Front.* **2023**, *10* (11), 2663–2669.
(28) Fu, S.; An, G.; Sun, H.; Luo, Q.; Hou, C.; Xu, J.; Dong, Z.; Liu, J. Laterally Functionalized Pillar[5]Arene: A New Building Block for Covalent Self-Assembly. *Chem. Commun.* **2017**, *53* (64), 9024–9027.
(29) Han, B.; Zhu, L.; Wang, X.; Bai, M.; Jiang, J. Conformation-Controlled Emission of AIE Luminogen: A Tetraphenylethene Embedded Pillar[5]Arene Skeleton. *Chem. Commun.* **2018**, *54* (7), 837–840.
(30) Meichsner, E.; Nierengarten, I.; Holler, M.; Chessé, M.; Nierengarten, J.-F. A Fullerene-Substituted Pillar[5]Arene for the Construction of a Photoactive Rotaxane. *Helv. Chim. Acta* **2018**, *101* (6), e1800059.
(31) Chen, Z-Z.; Cao, D.R. Synthesis of Bis(4-Bromo-2,5-Dialkoxyphenyl)Methane and Its Analogues. *Chin. J. Org. Chem.* **2010**, *30* (11), 1742–1744.
(32) Tian, X.; Zuo, M.; Niu, P.; Velmurugan, K.; Wang, K.; Zhao, Y.; Wang, L.; Hu, X.-Y. Orthogonal Design of a Water-Soluble *Meso* -Tetraphenylethene-Functionalized Pillar[5]Arene with Aggregation-Induced Emission Property and Its Therapeutic Application. *ACS Appl. Mater. Interfaces* **2021**, *13* (31), 37466–37474.
(33) Bai, Z.; Velmurugan, K.; Tian, X.; Zuo, M.; Wang, K.; Hu, X.-Y. Tetraphenylethylene-Embedded Pillar[5]Arene-Based Orthogonal Self-Assembly for Efficient Photocatalysis in Water. *Beilstein J. Org. Chem.* **2022**, *18*, 429–437.
(34) Wang, K.; Zhang, R.; Song, Z.; Zhang, K.; Tian, X.; Pangannaya, S.; Zuo, M.; Hu, X.-Y. Dimeric Pillar[5]Arene as a Novel Fluorescent Host for Controllable Fabrication of Supramolecular Assemblies and Their Photocatalytic Applications. *Adv. Sci.* **2023**, *10* (9), 2206897.
(35) Zhang, T.; Wang, K.; Huang, X.; Jiao, J.; Hu, X.-Y. Pillar[5]Arene Derivatives Embedded with Aggregation-Induced Emission Luminogens and Their Fluorescence Regulation. *Chem. Eur. J.* **2023**, *29* (19), e202203738.
(36) Fu, S.; Zhang, Y.; Guan, S.; Huang, Q.; Wang, R.; Tian, R.; Zang, M.; Qiao, S.; Zhang, X.; Liu, S.; Fan, X.; Li, X.; Luo, Q.; Hou, C.; Xu, J.; Dong, Z.; Liu, J. Reductive-Responsive, Single-Molecular-Layer Polymer Nanocapsules Prepared by Lateral-Functionalized Pillar[5]Arenes for Targeting Anticancer Drug Delivery. *ACS Appl. Mater. Interfaces* **2018**, *10* (17), 14281–14286.
(37) Fu, S.; Li, F.; Zang, M.; Zhang, Z.; Ji, Y.; Yu, X.; Luo, Q.; Guan, S.; Xu, J.; Liu, J. Diselenium-Containing Ultrathin Polymer Nanocapsules for Highly Efficient Targeted Drug Delivery and Combined Anticancer Effect. *J. Mater. Chem. B* **2019**, *7* (32), 4927–4932.
(38) Li, F.; Zang, M.; Hou, J.; Luo, Q.; Yu, S.; Sun, H.; Xu, J.; Liu, J. Cascade Catalytic Nanoplatform Constructed by Laterally-Functionalized Pillar[5]Arenes for Antibacterial Chemodynamic Therapy. *J. Mater. Chem. B* **2021**, *9* (25), 5069–5075.
(39) Ling, L.; Jiang, S.; Lan, S.; Zhang, C.; Ma, D. Step-Growth Cyclo-Oligomerization for the Preparation of Functionalized Pillar[6]Arenes with Alternating Methylene Bridge Substitutions. *Org. Lett.* **2021**, *23* (23), 9327–9331.
(40) Ma, Y.; Zhang, Z.; Ji, X.; Han, C.; He, J.; Abliz, Z.; Chen, W.; Huang, F. Preparation of Pillar[n]Arenes by Cyclooligomerization of 2,5-Dialkoxybenzyl Alcohols or 2,5-Dialkoxybenzyl Bromides. *Eur. J. Org. Chem.* **2011**, *2011* (27), 5331–5335.
(41) Timmerman, P.; Verboom, W.; Reinhoudt, D. N. Resorcinarenes; Tetrahedron Report 390. *Tetrahedron*, **1996**, *52* (8), 2663–2704.
(42) Taylor, R.; Wood, P. A. A Million Crystal Structures: The Whole Is Greater than the Sum of Its Parts. *Chem. Rev.* **2019**, *119* (16), 9427–9477.
(43) Jie, K.; Zhou, Y.; Li, E.; Zhao, R.; Huang, F. Separation of Aromatics/Cyclic Aliphatics by Nonporous Adaptive Pillararene Crystals. *Angew. Chem. Int. Ed.* **2018**, *57* (39), 12845–12849.
(44) Zuilhof, H.; Sue, A. C.-H.; Escorihuela, J. On the Stability and Formation of Pillar[*n*]Arenes: A DFT Study. *J. Org. Chem.* **2021**, *86* (21), 14956–14963.
(45) Zuilhof and co-workers calculated that a "1 ring flipped" conformation of pillar[6]arene was 26 kJ mol^{-1} lower in energy than the pillar form in the gas phase and a "2 ring flipped" conformation was 38 kJ mol^{-1} lower, see Reference 44.
(46) Fan, J.; Deng, H.; Li, J.; Jia, X.; Li, C. Charge-Transfer Inclusion Complex Formation of Tropylium Cation with Pillar[6]Arenes. *Chem. Commun.* **2013**, *49* (56), 6343.
(47) Han, C.; Ma, F.; Zhang, Z.; Xia, B.; Yu, Y.; Huang, F. DIBPillar[*n*]Arenes (*n* = 5, 6): Syntheses, X-Ray Crystal Structures, and Complexation with *n* -Octyltriethyl Ammonium Hexafluorophosphate. *Org. Lett.* **2010**, *12* (19), 4360–4363.
(48) We note that Ma and co-workers saw some reaction of benzaldehyde with 1,4-dimethoxybenzene using related conditions (trifluoroacetic Acid and $BF3{\cdot}OEt_2$ in DCM), giving a dimer in 33% yield, a 5% yield of trimer and other oligomeric species over a 7 day reaction (See Reference 39). Under our conditions (methanesulfonic acid in 1,2-DCE), we observed very little reaction with the major products being unreacted **1** and benzaldehyde.
(49) Ogoshi, T.; Aoki, T.; Kitajima, K.; Fujinami, S.; Yamagishi, T.; Nakamoto, Y. Facile, Rapid, and High-Yield Synthesis of Pillar[5]Arene from Commercially Available Reagents and Its X-Ray Crystal Structure. *J. Org. Chem.* **2011**, *76* (1), 328–331.
(50) Swirepik, O.; Smith, J. N.; White, N. G. Balancing on a Knife's Edge: Studies on the Synthesis of Pillar[6]Arene Derivatives. *J. Org. Chem.* **2023**, *88* (13), 8310–8315.
(51) Holler, M.; Allenbach, N.; Sonet, J.; Nierengarten, J.-F. The High Yielding Synthesis of Pillar[5]Arenes under Friedel–Crafts Conditions Explained by Dynamic Covalent Bond Formation. *Chem. Commun.* **2012**, *48* (20), 2576–2578.
(52) Xiong, W.; Huang, W.; Zhang, M.; Hu, P.; Cui, H.; Zhang, Q. Pillar[5]Quinone–Carbon Nanocomposites as High-Capacity Cathodes for Sodium-Ion Batteries. *Chem. Mater.* **2019**, *31* (19), 8069–8075.
(53) Frisch, M. J.; Trucks, G. W.; Schlegel, H. B.; Scuseria, G. E.; Robb, M. A.; Cheeseman, J. R.; Scalmani, G.; Barone, V.; Petersson, G. A.; Nakatsuji, H.; Li, X.; Caricato, M.; Marenich, A. V.; Bloino, J.; Janesko, B. G.; Gomperts, R.; Mennucci, B.; Hratchian, H. P.; Ortiz, J. V.; Izmaylov, A. F.; Sonnenberg, J. L.; Williams; Ding, F.; Lipparini, F.; Egidi, F.; Goings, J.; Peng, B.; Petrone, A.; Henderson, T.; Ranasinghe, D.; Zakrzewski, V. G.; Gao, J.; Rega, N.; Zheng, G.; Liang, W.; Hada, M.; Ehara, M.; Toyota, K.; Fukuda, R.; Hasegawa, J.; Ishida, M.; Nakajima, T.; Honda, Y.; Kitao, O.; Nakai, H.; Vreven, T.; Throssell, K.; Montgomery Jr., J. A.; Peralta, J. E.; Ogliaro, F.; Bearpark, M. J.; Heyd, J. J.; Brothers, E. N.; Kudin, K. N.; Staroverov, V. N.; Keith, T. A.; Kobayashi, R.; Normand, J.; Raghavachari, K.; Rendell, A. P.; Burant, J. C.; Iyengar, S. S.; Tomasi, J.; Cossi, M.; Millam, J. M.; Klene, M.; Adamo, C.; Cammi, R.; Ochterski, J. W.; Martin, R. L.; Morokuma, K.; Farkas, O.; Foresman, J. B.; Fox, D. J. Gaussian 16 Rev. C.01, 2016.
(54) Kesharwani, M. K.; Brauer, B.; Martin, J. M. L. Frequency and Zero-Point Vibrational Energy Scale Factors for Double-Hybrid Density Functionals (and Other Selected Methods): Can Anharmonic Force Fields Be Avoided? *J. Phys. Chem. A* **2015**, *119* (9), 1701–1714.
(55) Cowieson, N. P.; Aragao, D.; Clift, M.; Ericsson, D. J.; Gee, C. H.; Mudie, N.; Panjikar, S.; Price, J. R.; Riboldi-Tunnicliffe, A.; Williamson, R.; Caradoc-Davies, T. MX1: A Bending-Magnet Crystallography Beamline Serving Both Chemical and Macromolecular Crystallography Communities at the Australian Synchrotron. *J. Synchrotron Radiat.* **2015**, *22*, 187–190.